Colloid Polym Sci (2011) 289:1609–1615
DOI 10.1007/s00396-011-2475-z

SHORT COMMUNICATION

Fast dynamic wetting of polymer surfaces by miscible and immiscible liquids

Pranesh Muralidhar · Elmar Bonaccurso · Günter K. Auernhammer · Hans-Jürgen Butt

Received: 27 April 2011 / Accepted: 16 June 2011 / Published online: 12 July 2011

Abstract The initial stages of spontaneous spreading of a solvent drop (toluene) on the surface of a soluble polymer (polystyrene) have been studied with a high-speed camera. For drops of 1–4 μL volume, the increase in contact radius r can be described by a power law $r \propto t^{\alpha}$, with the spreading exponent α=0.50 and for the first ≈8 ms. Thereafter, the three-phase contact line was pinned leading to a macroscopic static contact angle of Θ_0=12–15°. The insoluble liquids ethanol (α=0.47, Θ_0=0) and water (α=0.35, Θ_0=90°) showed a slower spreading. We attribute the fast spreading of toluene to the strong interaction with the polymer, like in reactive wetting. The finite macroscopic contact angle indicates the formation of a ridge by softening of polystyrene due to permeated toluene and the subsequent plastic deformation by the surface tension of the liquid. This interpretation is supported by experiments on polymers grafted from a silicon wafer. Toluene completely wets polymer brush surfaces. Transport of toluene through the vapor phase plays a significant role.

Keywords Polystyrene · Toluene · Contact angle · Spreading · Kinetics · Polymer brush

P. Muralidhar · G. K. Auernhammer · H.-J. Butt (✉)
Max Planck Institute for Polymer Research,
Ackermannweg 10,
55128 Mainz, Germany
e-mail: butt@mpip-mainz.mpg.de

E. Bonaccurso
Center of Smart Interfaces, Technical University Darmstadt,
Petersenstr. 32,
64287 Darmstadt, Germany

Introduction

Spontaneous spreading of liquids is relevant in a number of processes like soldering, printing, and coating. The dynamics of spontaneous wetting has been studied extensively [1–5]. When a liquid drop is placed on a hard, inert surface the interfacial tensional forces cause the drop to spread. The gradient of curvature of the liquid surface and thus the capillary [6] (Laplace) pressure between the center and the periphery of the drop cause the drop to expand. The contact radius increases with time t as [7, 8]

$$r = r_0 t^{\alpha} \tag{1}$$

Here, α is the spreading exponent and r_0 is a coefficient depending on the initial conditions and the materials properties. Depending on the effect limiting the speed of wetting, the spreading exponent varies. Typically, in the first few milliseconds the inertia of the liquid mass transported limits the spreading speed. In this initial regime and for low static contact angles ($\Theta_0 << 90°$) α=0.5 [9–11]. In the second regime, wetting is limited by viscous hydrodynamic effects. Spreading slows down and α=0.1–0.14 [12–16], depending also on drop size. Small spherical drops seem to follow a power law with α=0.1 [12–16]. For liquid with a viscosity η above 0.05 Pa s, the viscous regime dominates right from the beginning [9]. When the drop has reached a contact radius of typically 1 cm or larger gravitation becomes the dominant force driving the expansion of the liquid. Then $\alpha \approx 0.125$ [13].

While the spontaneous wetting in the viscous regime has been studied extensively, it is only recently that researchers have started looking at the inertial phase of wetting. Soboleva et al. could show experimentally the transition from inertial to

viscous spreading of a liquid drop on a solid surface and derive a model for describing the transition taking place in the first milliseconds of drop spreading [9, 17]. They verified that for liquids of low viscosity (η<0.05 Pa s) in the inertial regime the wetting speed is indeed independent on the viscosity and α=0.5 for polar and non-polar liquids.

Biance et al. [11] investigated the first milliseconds of spreading of a water drop on a glass slide using a high-speed camera. They confirmed that in the inertial phase and for Θ_0=0 the drop contact radius increases with a square root dependence on time (α=0.5). Similar results had also been predicted [10, 18] and observed for coalescing drops [19] and drops coalescing with a pool of liquid [20]. These experiments indicated that a drop of a liquid with Θ_0=0 shows much the same dynamics as two coalescing drops or a drop coalescing in a pool.

Bird et al. [21] investigated this issue by preparing surfaces of varying wettability and focused on the first few milliseconds of spreading of a water–glycerol mixture drop with a high-speed camera. The time was rescaled by the Rayleigh time scale $\tau = \sqrt{\rho R^3/\gamma}$, and the contact radius r was rescaled with the initial radius R of the drop before touching the surface. Here, ρ is the density of the liquid and γ denotes its surface tension. They confirmed the power law of Eq. 1. However, the exponent α gradually dropped from 0.5 to around 0.3 when the wettability of the substrate became poorer, i.e., the exponent of the power law decreased with increasing Θ_0. Thus, the only factors affecting spreading in this initial fast regime were found to be the surface wettability and drop size, and thus inertial forces. Viscosity was found to play no role; the study was, however, limited to liquids with viscosities up to around 11 mPa s.

Here we report on the initial phase of wetting of a flat polystyrene surface by toluene, a good solvent for polystyrene. Unlike on an inert surface, the formation of a prewetting layer is unlikely because toluene would diffuse into the polystyrene after adsorption. Toluene drops wetting polystyrene have been studied in detail by Li et al. [22–24] and Bonaccurso et al. [25, 26]. They concentrated on the later stage after the drop had spread on the polystyrene. They let the drop evaporate in air and analyzed the microstructures that had been formed afterwards. Depending on the molecular weight of the polystyrene, different shapes of the evaporation structures developed. Analysis of the evaporation structures showed that toluene formed a finite contact angle with polystyrene. This is in contrast to expectation. Since polystyrene is soluble in toluene a contact angle of zero was expected. To understand the wetting behavior of a solvent on a soluble substrate, we performed wetting experiments of toluene drops on flat plates of polystyrene with different molecular weight of the polymer. For comparison, also the wetting of ethanol and water were analyzed. Ethanol (γ=22.1 mN/m, η=1.13 mPa s at 23 °C) has a surface tension close to toluene (γ=28.2 mN/m, η=0.57 mPa s). Water (γ=72.3 mN/m, η=0.95 mPa s) was chosen because it forms a high contact angle on the hydrophobic polystyrene (Θ_0=80–90°). The three liquids have dynamic viscosities of the same order of magnitude.

Materials and methods

Experimental setup

Liquid drops were placed on the solid substrate by a microliter syringe (Fig. 1). The needle of the syringe was either Teflon coated of outer diameter 260 μm or a borosilicate glass microtip. The diameter of the glass microtip could be tuned down to a few tens of micrometers by the procedure used to pull the glass capillary. This allowed making drops of different sizes. The substrate was placed on a vertical stage and illuminated from behind by a cold light source (Zeiss, KL2500) and a diffuser. The process was visualized with a high-speed camera (Photron SA1) which was inclined at an angle (below 5°) to the plane of the drop so as to also get the reflection of the drop on the substrate. The spreading process is captured as a movie with a frame rate of typically 36.000 fps. We use a macro-zoom optic (Navitar) that allowed for a spatial resolution of 6 μm. Experiments were carried out at 23±1 °C.

Materials

Polystyrene with molar masses M_W=26, 65, 210, and 560 kDa was synthesized by anionic polymerization. The polydispersity of all samples was 1.05 or better. To produce flat substrates, the polystyrene powder was compression molded at 175 °C. The powder was placed in a split mold and compressed by a hydraulic press at a defined force of 50 kN. An optional vacuum fitting was occasionally used, however, no difference was found in the quality of the samples. The diameter of the plates measured 25 mm, and

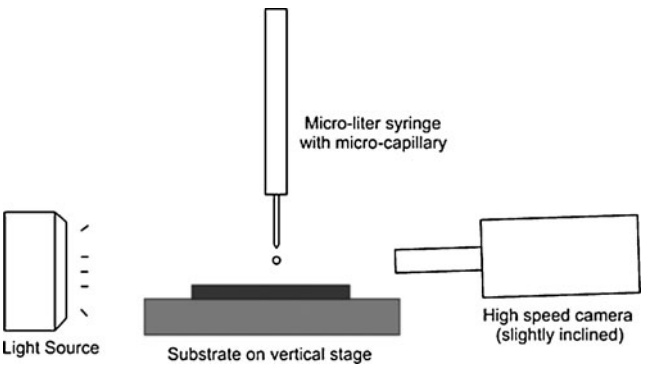

Fig. 1 Schematic diagram of the experimental setup

the thickness was 1 mm for all samples except the 26 kDa, where a thickness of 3 mm was used to avoid damaging the polymer plate by wrinkling. The molds were coated with Kapton sheets (Polyimide films, Dupont, USA) of diameter 25 mm. This was done to ensure a smooth surface of the polystyrene, which is essential to study wetting. Using the Kapton sheets usually imparted a root-mean-square roughness of 100–200 nm of no particular direction to the surface of the polystyrene plate, as was measured by scanning confocal microscopy (μSurf, Nanofocus AG, Germany). The polystyrene plates were cleaned in an ultrasonic bath of ethanol for around 10–15 min and then vacuum dried at 40–50 °C for a period of 15–20 min prior to the experiment.

Experiments were also carried out on polystyrene brushes. These brushes had a thickness of 15–20 nm and were end-grafted on one side onto silicon substrates. The cleaning procedure of the brushes was the same as that of the plates. The preparation of polymer brushes by a grafting from synthesis was described before [27]. Briefly, first naturally oxidized silicon wafers were immersed in a mixture of NH_3 (8 mL, 25%), H_2O_2 (8 mL, 35%) and Millipore water (100 mL) at 80–85 °C for 20–25 min. Afterwards, the wafers were rinsed with copious amounts of Millipore water and dried under nitrogen flow. Then the wafers were immersed in a mixture of dry toluene, triethylamine, and starter (25 mM) for 20 h. The wafer was removed from the starter solution and cleaned by extraction in dichloromethane. The starter, (3-(2-bromoisobutyryl)propyl)dimethyl chlorosilane, was synthesized following the procedure described in [28] and purified by distillation under reduced pressure. To prevent degradation by moisture, it was stored under argon atmosphere over silica–gel in a desiccator.

Brushes were synthesized by an ATRP reaction under protective argon in modified Schlenk flask that contained the silanised wafer, CuBr (13 and 26 mg), degassed anisole (10 mL), styrene (10 mL), and *N*,*N*,*N*′,*N*′,*N*″-pentamethyldiethylenetriamine (PMDETA, 38 and 19 μL, Aldrich, 99%). After stirring for 15 min under an argon atmosphere, ethyl 2-bromoisobutyrate (2-EiBBr, 26 and 13 μL, Aldrich, 98%) was added. The reaction mixture was then deoxygenated by three freeze/pump/thaw cycles and stirred at 90 °C. To remove bulk polymer, the wafer was extracted 24 h in a soxhlet apparatus. The bulk polymer was precipitated twice in methanol and dried. The resulting molar masses M_n were 20.6 and 23.9 kDa with a PDI of 1.17 and 1.28, respectively.

Image analysis and processing

Static contact angles were analyzed with a commercial software (FDS, OCA-20). For dynamic contact angles we developed an automatic analysis program, which calculated for each frame of the movie contact angle, contact radius, volume, and other drop parameters. The code was written in Matlab. The algorithm relies on good quality images with a uniform contrast over the area of interest. The images captured also include the reflection of the drop on the substrate (Fig. 2). The brightness is reduced in the image to reduce saturation and pick out more details. Then the movie is thresholded using *ImageJ* to obtain an image in black and white. This has only 2 pixel values 0 and 255, 255 representing the drop and 0 the background. To avoid complications, only the part where the drop meets the substrate was extracted. Image informations were exported as a matrix of intensities in ASCII format. The exported file essentially contains the coordinates of the drop shape. This file was given as input to the algorithm which outputs the relevant parameters of interest. For a quantitative analysis, the cross-section of the drop needs to meet the substrate at a single point; only experiments in which drops fulfilled this condition were analyzed. Time zero $t=0$ is taken as one frame before the formation of the liquid bridge with the substrate.

Results and discussion

Wetting of polystyrene

As soon as a toluene drop gets into contact with the polystyrene surface it forms a meniscus and the meniscus starts to expand (Fig. 2). While the drop is spreading, a capillary wave propagates along the drop surface. Spreading lasts approximately as long as the capillary wave takes

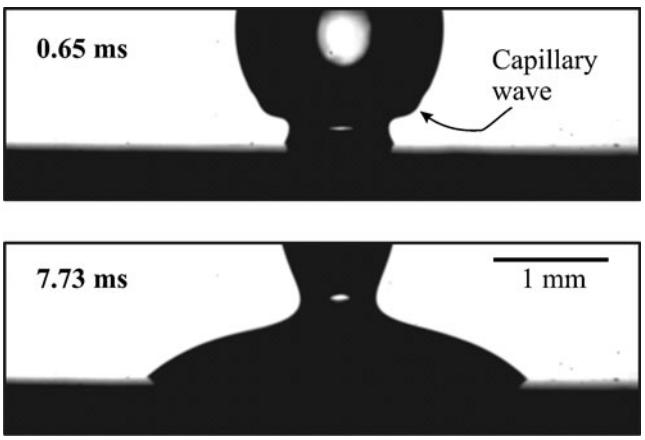

Fig. 2 Snapshots in time of a toluene drop spreading on the planar polystyrene (M_W=26 kDa). The first image was recorded 0.65 ms after contact, and the second image was recorded 7.73 ms after the first image. The capillary wave is seen to be traveling out from the point of contact over the drop to the micro-capillary

to propagate from the contact point to the top of the drop. When the capillary wave reached the top of the drop at the rim of the syringe it pinched off. After typically 8 ms the toluene drop is pinned at the periphery. It further evaporates with a pinned contact line and a decreasing contact angle. The apparent, static contact angle of toluene drops on polystyrene was 12–15°. "Static" refers to the contact angle reached after the initial spreading before a significant amount had evaporated. It did not depend on the molar mass of the polymer or on the initial drop size.

As reported in the literature on the spreading on undeformable, insoluble surfaces, we observed a fast and a slow wetting regime. The increase of the contact radius with time in the fast spreading regime could be described by Eq. 1. When plotting the contact radius versus time on a double logarithmic scale, straight lines were obtained (Fig. 3). For a better comparison of different liquids, we also show the normalized contact radius r/R versus the normalized time t/τ. For toluene a spreading exponent of $\alpha=0.50\pm0.014$ (standard deviation of the experimental values) was obtained, independent on molecular weight (Fig. 4). In normalized units, the power law described the results well for $t/\tau=0.1$ to 2. Afterwards, the slow regime started. A change in slope was observed in the plots of contact angle versus normalized time at $t/\tau=2$.

Ethanol spread slightly slower than toluene; its fast spreading could be described by an exponent $\alpha=0.47\pm0.01$. It finally spreads to a continuous film with zero contact angle.

Water was distinctly slower than toluene and ethanol, with an exponent $\alpha=0.36\pm0.01$. The static contact angle was 90°. The lower spreading exponents for water can be explained by the high static contact angle of water on polystyrene. A high static contact angle leads to a lower driving force for spreading, $\gamma(\cos\Theta_0-\cos\Theta)$, where Θ is the dynamic contact angle. It further leads to a reduced curvature and thus a reduced gradient in the Laplace pressure. It should also influence the entrained mass and the driving force for spreading. Bird et al. [21] found for water a value of $\alpha=0.35$ for $\Theta_0\approx100°$, which agrees with our results.

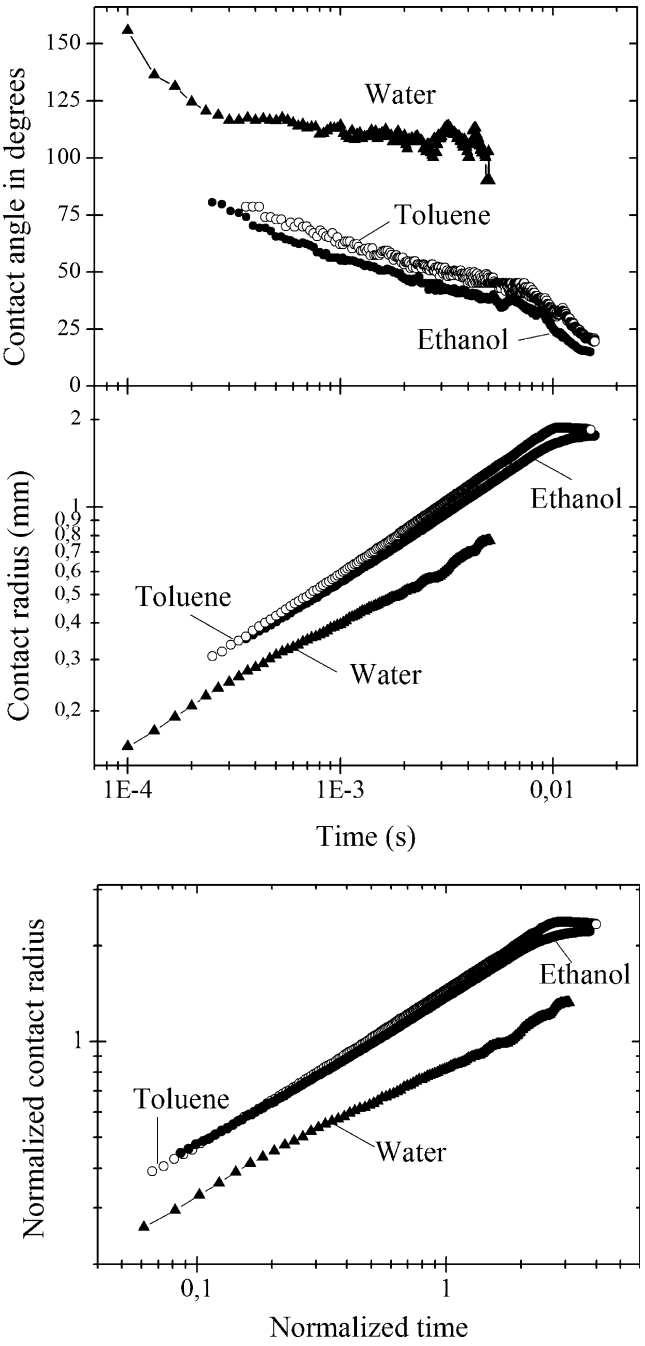

Fig. 3 Log–log plots of contact angle versus real time, contact radius versus real time, and normalized contact radius versus normalized time, respectively. The normalized radius is the radius r divided by the radius R of the hanging drop just before contact. The normalized time is the actual time divided by the Rayleigh time τ. The substrate for the experiments was a flat polystyrene plate of $M_W=69$ kDa. The initial drop radii in this particular experiment were $R=0.58$ mm (water) and $R=0.79$ mm (ethanol and toluene)

Wetting of polystyrene brushes

To further elucidate the reason for a finite contact angle of toluene on polystyrene, experiments were also performed with toluene and ethanol drops spreading on polystyrene brushes (Fig. 5). Polystyrene brushes cannot dissolve in the solvent but only swell since they are covalently attached to the surface with one end. The spreading of ethanol drops on polystyrene brushes did not show significant differences with respect to flat polystyrene substrates. Toluene drops, on the other hand, spread completely, and the static contact angle was zero. The wetting coefficients for the fast wetting regime, though, were the same as for bulk polystyrene ($\alpha=0.50$).

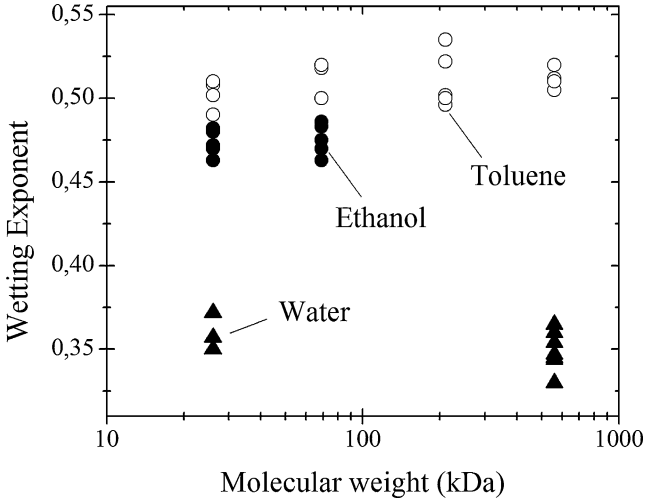

Fig. 4 Wetting exponents of toluene, ethanol, and water on polystyrene versus the molecular weight of the polystyrene

Fast spreading of toluene

The difference of the fast wetting velocity between toluene and ethanol on polystyrene could be explained by a mechanism similar to what is observed in reactive wetting of metal alloys at high temperatures ([29–31] and references therein). In such processes, like soldering or brazing, a liquid metal drop at high temperature (T>250 °C) wets another metal surface at lower temperature (room temperature). It has been observed that if the metals are miscible wetting proceeds much faster than if the metals are non-miscible. Based on experiments and simulations it has been postulated that wetting speeds directly dependent on dissolution kinetics. In general, reactions occurring between liquid and solid accelerate spreading. The gain in free energy due to a mixing is proposed to create an additional driving force for wetting [32]. This phenomenon seems to apply also for toluene on a polystyrene surface, in contrast to ethanol or water. The additional free energy comes from the high interaction parameter of polystyrene and toluene

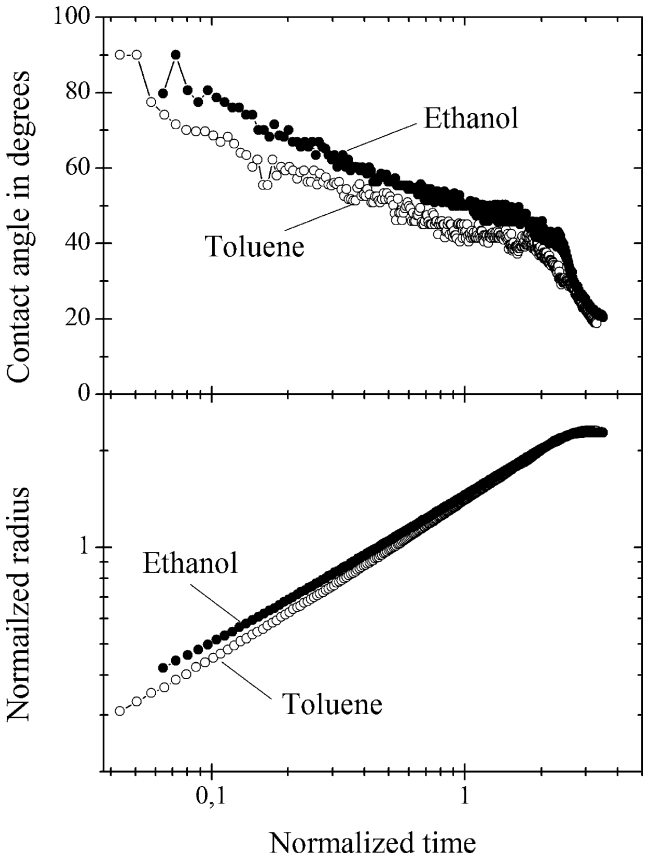

Fig. 5 Contact angle and normalized contact radius for toluene and ethanol spreading on polystyrene brushes of 26 kDa. The initial drop radii were R=0.79 mm

Ridge formation

Why does toluene not spread infinitely and form zero static contact angle? After the fast regime (t/τ>2), ethanol spreads out and finally completely wets the substrate, while toluene spreads out only to a certain finite macroscopic contact angle and then the contact line is pinned. We propose that the three-phase contact line is pinned because the polystyrene surface is softened by the toluene and a ridge is formed, like in the case of immiscible drops sitting on deformable substrates [33, 26, 34]. That such ridges form is evident from images of polystyrene surfaces after toluene drops had evaporated [22–24]. Ridges as high as several micrometers have been observed previously [25, 26, 34]. On the brushes, the deformation is limited to a few nanometers since the polymer chains cannot extend more. For a ridge to form, the toluene has to diffuse into the polystyrene to a sufficient concentration and depth. Then, the polystyrene/toluene mixture deforms plastically by the force caused by the vertical component of the surface tension of the liquid. These processes, diffusion and plastic deformation, have to be fast enough so that the three-phase contact line has not moved on before a ridge of sufficient size has formed.

The spreading speed of toluene on polystyrene just before pinning was 7.5 cm/s. If we estimate the lateral extension of the ridge to be of the order of 1 μm, the three-phase contact line crosses that distance in 13 μs. This time has to be related to the diffusion of toluene into polystyrene. For temperatures above the glass transition temperature of polystyrene of 100 °C and for high weight fractions of toluene, diffusion coefficients have been measured by various techniques (e.g., [35, 36]). Diffusion of toluene in polystyrene depends sensitively on the concentration of toluene. It is fast at high weight fractions of toluene. Experimental results for room temperature and low toluene content are rare and they differ significantly [37, 38]. At a

weight fraction of toluene below 0.1 and at room temperature diffusion is not even Fickian [39–42]. Krüger and Sadowski [40] report a diffusion coefficient of toluene in polystyrene at 30 °C and a weight fraction of 0.14 to be $D=2.8\times10^{-13}$ m^2/s. We take this as an upper limit for the diffusion of toluene with low toluene content at room temperature. In Δt=13 μs, toluene diffuses of the order of $\Delta x = \sqrt{6D\Delta t} = 5$ nm. This is not enough to soften the polystyrene sufficiently for ridge formation.

Transport through the vapor phase

Therefore, we conclude that there is an influence of diffusion of toluene vapor through air ahead of the spreading liquid. The toluene vapor is absorbed by the polystyrene, which increases the toluene content before the liquid actually wets the polystyrene. Toluene vapor in air has a diffusion coefficient of 8×10^{-6} m^2/s [23]. In 8 ms, the time after which a toluene drop is typically pinned, toluene vapor diffuses ≈0.6 mm. This is of the same order of magnitude as the contact radius of the drop. Furthermore, in the experiments the pipette with the toluene drop was slowly moved towards the polystyrene surface. Some toluene continuously evaporated. It was unavoidable that some toluene vapor adsorbed onto the polystyrene. This could have led to a softening of the polymer surface even before the liquid toluene got into contact with the polystyrene. We tested this possibility by letting a drop hang in air close to the surface for 30 s. No difference in spreading was observed. In another experiment, we exposed polystyrene to toluene vapor by placing a filter paper soaked with toluene close to the polymer surface in a closed beaker for 15–20 min. Then, we noticed a slight change in the speed of wetting. Hence, a long exposure to a high vapor pressure of toluene softens polystyrene sufficiently to alter the spreading process.

The absorption of toluene could be reduced by releasing the toluene drops from a certain height. When releasing toluene drops from a height of 10 mm onto the surface, the final contact angle was around 2–3° smaller than what was observed at small release heights. In these experiments, the spreading is, however, partially enforced by the increased inertia of the drop and not purely spontaneous. At the end of the fast regime, the droplet had spread to a greater extent because of the inertia of falling.

Possible dissolution effects

A possible alternative explanation of the line pinning is the following: polystyrene dissolves in toluene (in the case of the bulk polystyrene, not the brushes). Once it is dissolved, it starts to diffuse. It can get concentrated close to the three-phase contact line because of evaporation. Close to the three-phase contact line, the concentration of polystyrene might be high, which can lead to an increased viscosity of the spreading liquid. An increased viscosity slows down the wetting process, allowing evaporation to become even more dominant and finally stops the movement of the three-phase constant line. However, it is unlikely that dissolution plays an important role during the first ≈8 ms because dissolution and the diffusion coefficient of dissolved polystyrene in toluene depend sensitively on the molar mass. Neither the static contact angle nor the wetting exponent did, however, depend on the molar mass. In addition, the diffusion coefficient of polystyrene in toluene can be estimated from $D = 2.8 \times 10^{-8} M_W^{-0.55}$m^2/s [43]. With M_W=26 kDa we get a diffusion coefficient of 10^{-10} m^2/s. Thus, in the first 10 ms, a polymer chain diffuses not more than 2 μm. Furthermore, it seems unlikely that evaporation of toluene is sufficiently fast compared with the contact line speed to significantly enrich PS close to the contact line.

The surface tension of a polystyrene/toluene solution increases with the volume fraction of polystyrene according to γ=28.2 mN/m+5$\Phi^{1.3}$ [44], with Φ being the volume fraction of polystyrene in toluene. A process, called solutocapillarity, could enhance spreading. Due to solvation of polystyrene at the drop rim, the surface tension there becomes higher, while at the top of the drop it remains low. The difference could be up to $\Delta\gamma\approx1$ mN/m for concentrated solutions. This effect is even enhanced, when evaporation sets in. Drops with so small contact angle evaporate predominantly from the rim. The temperature decrease due to the loss of latent heat would further increase the surface tension gradient. This difference causes a convective Marangoni flow from the top of the drop to the three-phase contact line. The additional convective velocity can be estimated by $dr/dt \approx \Delta\gamma \sin\Theta_0/\eta\approx0.3$ m/s, with $\Theta_0\approx12°$, $\Delta\gamma\approx1$ mN/m, and $\eta\approx0.57$ mPa s [45, 46]. This value is certainly overestimated since at this late spreading stage the rim velocity is below 10 mm/s. It tells us, however, that there might be an additional convective flow inside the drop during the late stages of wetting.

Conclusions

The dynamics of wetting of a solvent on a soluble polymer has been studied for combinations of toluene on polystyrene substrates of different molecular weights and compared with non-soluble liquids (ethanol and water). For drops of initially 1–4 μL volume, spreading of toluene drops can be described by a power law with a spreading exponent of 0.5. Ethanol and water show lower spreading exponents. Toluene is observed to wet the polystyrene faster than ethanol, most probably by the mechanism of *reactive wetting* because of its affinity to the substrate. The apparent

static contact angle reached after ≈10 ms was 12–15°. For polymer brushes, instead, complete wetting was observed. The pinning in the case of bulk polymer is interpreted by the formation of a ridge formed by the polymer. For ridge formation, transport of toluene through the vapor phase and subsequent adsorption by the polystyrene is a prerequisite.

Acknowledgments HJB thanks the DFG for financial support of project Bu 1556/27. We thank Thomas Wagner, Jürgen Thiel, and Gunnar Kircher for synthesizing the polystyrene and the brushes. We further thank Daniela Fell, Chuanjun Liu, Valentina Marcon, and Nico van der Vegt for helpful discussions.

References

1. Blake TD (2006) J Colloid Interface Sci 299:1
2. Starov VM, Velarde MG, Radke CJ (2007) Wetting and Spreading Dynamics. CRC Press, London
3. Courbin L, Bird JC, Reyssat M, Stone HA (2009) J Phys Condens Matter 21:464127
4. Bonn D, Eggers J, Indekeu J, Meunier J, Rolley E (2009) Rev Modern Physics 81:739
5. Wei Y, Rame E, Walker LM, Garoff S (2009) J Phys Condens Matter 21:464126
6. Monteux C, Tay A, Narita T, de Wilde Y, Lequeux F (2009) Soft Matter 5:3713
7. Lelah MD, Marmur A (1981) J Colloid Interface Sci 82:518
8. Joanny JF (1987) Physicochem Hydrodyn 9:183
9. Soboleva OA, Raud EA, Summ BD (1991) Kolloidnyi Zhurnal 53:1106
10. Duchemin L, Eggers J, Josserand C (2003) J Fluid Mech 487:167
11. Biance AL, Clanet C, Quéré D (2004) Phys Rev E 69:016301
12. Tanner LH (1979) J Phys D 12:1473
13. Cazabat AM, Cohen Stuart MA (1986) J Phys Chem 90:5845
14. Ausserré D, Picard AM, Léger L (1986) Phys Rev Lett 57:2671
15. Chen JD (1988) J Colloid Interface Sci 122:60
16. Seaver AE, Berg JC (1994) J Appl Polymer Sci 52:431
17. Soboleva OA, Summ BD, Raud EA (1989) Kolloidnyi Zhurnal 51:1204
18. Eggers J, Lister JR, Stone HA (1999) J Fluid Mech 401:293
19. Wu M, Cubaud T, Ho C (2004) Phys Fluids 16:L51
20. Thoroddsen ST, Qian B, Etoh TG, Takehara K (2007) Phys Fluids 19:072110
21. Bird JC, Mandre S, Stone HA (2008) Phys Rev Lett 100:234501
22. Li G, Graf K, Bonaccurso E, Golovko DS, Best A, Butt H-J (2007) Macromol Chem Phys 208:2134
23. Li G, Butt H-J, Graf K (2006) Langmuir 22:11395
24. Li GF, Graf K (2009) Phys Chem Chem Phys 11:7137
25. Bonaccurso E, Butt HJ, Hankeln B, Niesenhaus B, Graf K (2005) Appl Phys Lett 86:124101
26. Pericet-Camara R, Best A, Nett S, Gutmann J, Bonaccurso E (2007) Optics Express 15:9877
27. Bumbu GG, Kircher G, Wolkenhauer M, Berger R, Gutmann JS (2004) Macromol Chem Phys 205:1713
28. Ramakrishnan A, Dhamodharan R, Rühe J (2002) Macromol Rapid Commun 23:612
29. Webb EB, Crest GS (2002) Scripta Mater 47:393
30. Yin L, Murray BT, Su SS Y, Efraim Y, Taitelbaum H, Singler TJ (2009) J Phys Condens Matter 21:464130
31. Saiz E, Benhassine M, de Coninck J, Tomsia AP (2010) Scripta Mater 62:934
32. Sobczak N, Singh M, Asthana R (2005) Current Opinion Solid State Materials Sci 9:241
33. Shanahan MER (1988) J Phys D 21:981
34. Pericet-Camara R, Best A, Butt HJ, Bonaccurso E (2008) Langmuir 24:10565
35. Duda JL, N YC, Vrentas JS (1979) J Appl Polymer Sci 23:947
36. Pickup S, Blum FD (1989) Macromolecules 22:3961
37. Gall TP, Kramer EJ (1991) Polymer 32:265
38. Gupper A, Chan KLA, Kazarian SG (2004) Macromolecules 37:6498
39. McDonald PJ, Godward J, Sackin R, Sear RP (2001) Macromolecules 34:1048
40. Krüger KM, Sadowski G (2005) Macromolecules 38:8408
41. Zhang R, Graf K, Berger R (2006) Appl Phys Lett 89:223114
42. Müller-Buschbaum P, Baur E, Maurer E, Cubitt R (2006) Physica B 385–386:703
43. Min G, Savin D, Gu Z, Patterson GD, Kim SH, Ramsay DJ, Fishman D, Ivanov I, Sheina E, Slaby E, Oliver J (2003) Intern J Polymer Anal Character 8:187
44. Ober R, Paz L, Taupin C, Pincus P, Boileau S (1983) Macromolecules 16:50
45. Camel D, Tison P, Garandet JP (2002) Eur Phys J AP 18:201
46. Kozlova O, Voytovych R, Protsenko P, Eustathopoulos N (2010) J Mater Sci 45:2099